

Monitoring the drilling process of carbon fibre laminates using acoustic emission

Mark J Eaton*, Davide Crivelli, Robert Williams, Carlton Byrne

Cardiff University, Cardiff School of Engineering, The Parade, CF24 3AA, Cardiff, United Kingdom

* eatonm@cardiff.ac.uk

Abstract

This work aims to apply Acoustic Emission to monitor the drilling process in carbon fibre laminates.

Continuous Acoustic Emission data is captured over the entire drilling process of a through hole.

The use of continuous acoustic emission data acquisition allows the identification of lower frequency periodic temporal features related to the cutting process. A new approach to data analysis is presented that utilises an enveloping technique to study these periodic phenomena and show that they correlate to changes in cutting regime as tool wear advances and hole quality reduces. This analysis of Acoustic Emission data is supported by the measurement of tool temperature, thrust force and the assessment of hole quality.

Results show that Acoustic Emission activity is correlated to changes in the cutting process, and a correlation between tool wear and Acoustic Emission is observed. This correlation has been confirmed by corresponding increases in thrust force and drill temperature, with a consequent decrease in the observed hole quality.

Keywords: Laminates; Process monitoring; Acoustic Emission; Machining

1 Introduction

Industrial uptake of carbon fibre composites has accelerated significantly in recent years and such materials are now widely used in large and safety-critical structures [1]. A particular example is the aerospace industry, where modern aircraft comprise of approximately 50% carbon fibre by weight [2,3]. Although moulded to their final desired shape, composite components still require edge trimming to achieve final dimensional tolerances and drilling and bolting is also still the preferred joining method in aerospace (adhesive bonding requires such rigorous process control that achieving reliability is prohibitively expensive).

The machining of carbon fibre composites is far from straightforward. Their laminated nature means that out-of-plane stresses can lead to delamination, which significantly reduce strength and fatigue life. In addition, carbon fibre is highly abrasive, meaning tool wear is extremely high. Current approaches to establishing and optimizing drilling parameters rely on dimensional tolerance, surface roughness and induced damage (determined by NDT) [4–6]. Tool life must be set at a conservative level, to account for the variability in operating conditions and usable life seen from tool to tool. The expensive tooling required (~£10/m for edge trimming and ~£1/hole for drilling [7]) and the number of machining actions needed (~16,000 holes per wing set (6 spars) and ~55,000 holes in total to complete assembly [8]) makes this a very expensive process. Hence, even small increases in useable tool life could make a significant impact on machining costs. For this reason, there is interest in in-process monitoring techniques for drilling that can provide an indication of tool wear.

This paper investigates the use of continuous acoustic emission (AE) as a monitoring tool for hole drilling in carbon fibre composite laminates. The AE technique enables the capture of high frequency energy emitted by the cutting processes. This energy is the fundamental source of the lower frequency vibration often observed in thrust force and vibration data, which have been investigated for monitoring drilling processes [9–14]. This technique improves fundamental understanding of the underlying phenomena and provides more sensitive analysis of changing process conditions. A new approach is presented, whereby continuous AE wavestreams are captured throughout the entire drilling process. Time-frequency analysis has been developed to provide detailed interpretation of the acquired data and an enveloping approach captures low frequency periodicity resulting from the cutting process. The AE data is compared with thrust force, temperature and hole dimensional tolerance to demonstrate that changes in the cutting process are effectively tracked. It is envisaged that an effective monitoring tool for machining activities would facilitate a shift to condition-based tool replacement, allowing full use of usable tool life and significant cost savings.

2 State of the Art

2.1 Tool wear

Tool wear during the machining of any medium is generally detrimental to part quality and tolerance. In metals this manifests as flank wear and leads to increased cutting forces. In carbon fibre reinforced polymers (CFRP) the highly abrasive fibres more commonly lead to gradually increasing and evenly distributed wear along the entire cutting edge. Therefore, Faraz et al. [8] proposed the wear metric of ‘cutting edge rounding’ (CER) for drilling of CFRP laminates. CER (i.e.

wear) has subsequently been strongly correlated with increases in cutting forces [15–17] and others have correlated wear more generally to increases in cutting forces [5,6,8,14,18–23]. Other undesirable effects have also been correlated to tool wear, such as loss of hole tolerance, reduction in surface finish and an increase in uncut fibres [20,24,25].

Increased cutting forces are particularly problematic in CFRP laminates. The induced interlaminar stresses lead to push-out delamination (Figure 1) when the thrust force exceeds a critical value for inter-ply bond strength [26]. The inter-ply bond strength also varies with material type, ply orientations and temperature [27]. Push-out delamination size can reach up to 2-3 times that of hole size [28–31] and has been shown to reduce bending strength by up to 20% in CFRP [29] and tensile strength by up to 10% in GFRP [32].

The temperatures during dry drilling actions in fibre reinforced laminates are observed to be high, due to the poor thermal conductivity of the matrices [22,33–37] and have been shown to increase with tool wear (CER) [25,38]. In most cases temperatures have exceeded the matrix glass transition temperature (t_g), which reduces interlaminar strength (reducing critical load for push-out delamination) and reduces support for fibres being cut (increasing fibre pull out and fibre bending). In severe cases thermal degradation has been observed.

The observed correlations of tool wear with increases in cutting forces, induced damage and temperature, as well as reductions in hole quality highlights the challenge of drilling in fibre reinforced laminates. It also reinforces the challenge of extending tool life based on tool condition, hence the desire to find effective monitoring tools for drilling processes.

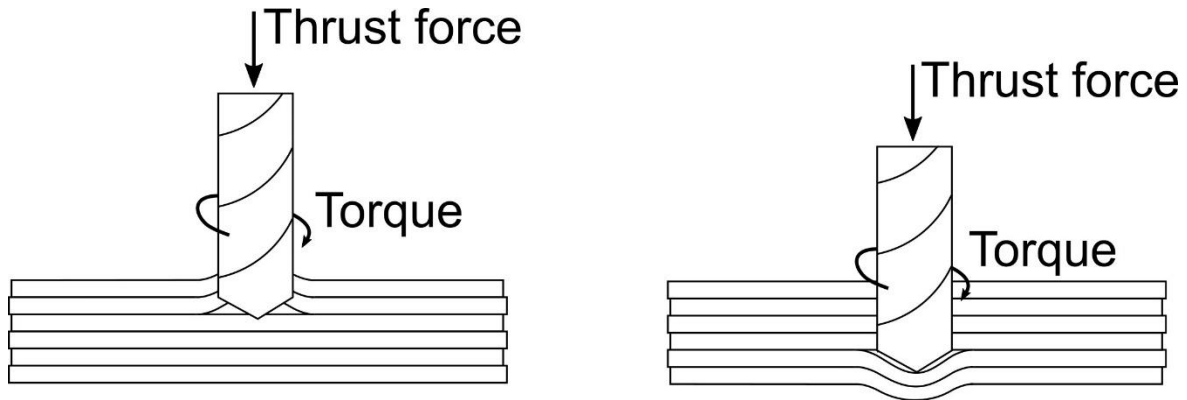


Figure 1: mechanisms of pull-up (left) and push-out (right) delaminations during composite drilling

2.2 Tool condition monitoring

Extensive reviews by Jantunen [9], Ambhore et al [10], Serin et al [11], and Kuntoglu et al [12] have covered approaches to tool condition monitoring, focussed on cutting in metals. The reported techniques include: monitoring cutting forces, torques and spindle power/current as well as vibration, sound and acoustic emission (AE).

The use of cutting forces and spindle current/power is commonly reported in studies of cutting in composite materials [5,6,14–16,18–22], but their oscillatory nature makes determining a reliable maximum challenging. Some researchers have used the oscillatory nature of the force signals to their advantage, showing the frequency is related to multiples of the cutting-edge pass frequency and were able to relate this to changes in CER and cutting conditions [14,39].

The vibration frequencies recorded during cutting operations are highly dependent on work piece and tool vibration modes, which are not directly linked to cutting and can change from part to part

[12]. Zhu et al [13] were therefore only able to predict tool condition with 80% accuracy using artificial neural networks (ANN) based on RMS levels of vibration signals and the RMS of decomposed frequency bands. Kuntoglu and Saglam [40] compared vibration, acoustic emission, motor current, temperature and cutting forces with tool wear during turning of medium carbon steel and concluded that AE and temperature were the most effective indicators of tool wear. Similarly, Mohring et al [15] compared vibration, electric power, thrust force, torque, airborne acoustics and acoustic emission (AE) for monitoring tool wear during milling of CFRP laminates. They also concluded that AE was the most sensitive to changes in tool wear (CER) and the median amplitude was shown to reduced in magnitude as tool wear increased. The higher sensitivity of AE is expected as the high frequency range considered (20kHz – 1 MHz) derives from microscale events such as cracks, plastic deformation and friction (i.e. the fundamental mechanisms of material removal) which cause sudden strain/stress field redistribution [41]. It is less expected that the time averaged AE amplitude would decrease with wear, particularly because vibration amplitude is seen to simultaneously increase as cutting quality reduces [15]. However, similar behaviour has been observed by other researchers when considering the RMS level of AE signals from machining of composite materials [42–46] and this has also been corroborated by the current authors [20,21].

Time averaging AE signals can, however, miss details occurring on a short temporal scale within the transients, that may provide further insight on the cutting regime. Instead, Zarif Karimi et al [47] studied the frequency content of burst type AE during drilling of GFRP samples in an attempt to characterize damage mechanisms. However, Maillet et al [48] and Eaton et al [49] have robustly shown that AE frequency is dominated by propagation and sensor transfer function. Additionally,

burst type AE is not relevant to drilling, where the length of a drilling action is significantly long (relative to a typical AE burst duration) such that the process is considered continuous.

Modern AE acquisition systems allow continuous AE transients to be stored, meaning drilling processes can be studied in greater detail. Mascaro et al [50] initially investigated continuous AE transients capture in carbon fibre/titanium stacks. Their data acquisition was limited to 7.9ms at the required 2MHz frequency, so only 26° of tool rotation could be analysed. They utilised Short Time Fourier Transform (STFT) analysis of the acquired signals which is not well suited to such short acquisition lengths. For the reported signal lengths a frequency resolution of ~130Hz can be expected, which is not sufficient to capture phenomena related to tool pass frequencies of ~20Hz. Mohring et al [15,51] and Kimmelman et al [52] collected continuous AE signals that capture the whole drilling action in CFRP/titanium stacks. They showed by STFT analysis that spectral content of the signals varies at different positions in the stack (i.e. in different materials). However, they don't discussed correlation to wear and considered only high frequencies (100s kHz) which are too high to capture cutting edge pass frequencies. Rimpault et al [53] captured continuous AE signals of whole drilling actions in CFRP laminates. The sample rate they used was very low for AE acquisition (48kHz) but they did identify periodic features corresponding to tool pass frequencies. They also assessed signal complexity by fractal analysis and showed that fractal index reduced with increasing wear.

Monitoring drilling actions in composite laminates using AE has shown good sensitivity to tool wear with a clear correlation between reducing signal amplitude (RMS) and increasing tool wear.

However, the underlying mechanism for this correlation has not been explained. Continuous AE

acquisition has demonstrated potential to provide greater detail and can capture temporal features related to the cutting process. However, the work presented thus far has not fully explored these temporal features or correlated them robustly to process conditions.

In this work continuous AE data acquisition is utilised to capture the entire drilling process in CFRP laminates. An enveloping technique is used to identify and analyse lower frequency periodic features, whilst maintaining the sensitivity of high frequency AE acquisition. This allows consideration of lower frequency phenomenon whilst avoiding component/tool vibrational frequencies. Tool wear was monitored indirectly through highly correlated features of thrust force and hole tolerance. Analysis of enveloped frequency bands shows more sensitive correlation of AE with tool condition. Data interpretation is supported by tool temperature measurement, which helps identify the mechanisms for changes in cutting regime and recorded AE amplitude, brought about by tool wear.

3 Experimental design

3.1 Methodology

The intention of this work is not to study the effects of tool, material or process related parameters on the process loads, induced damage or hole quality. The aim is to establish a wear process of tools used to drill CFRP laminates, to validate wear through established metrics (i.e. Thrust force, temperature, hole quality) and to correlate wear to recorded AE. As such the experiment is kept as simple as possible. Given that the dominant tool wear mechanism of cutting-edge rounding is geometry independent [8], a standard twist bit geometry was selected. A cutting speed of 44 m/min

(1573 rpm) was selected to sit within the conventional drilling regime specified by Liu et al [6], i.e. <100 m/min (generally rotational speeds less than <8000 rpm). To correlate AE with wear over different cutting conditions, two feed rates of 0.0326 mm/rev and 0.0508 mm/rev were selected, as feed rate has been shown to correlate strongly to wear [6]. These values of cutting speed and feed rate are also similar to those used by Faraz et al [8] in their study on CER (cutting speed 50 m/min, feed rate 0.1 mm/rev). A tool material of High-Speed Steel (HSS) was selected, as this exhibits high wear rates when drilling CFRP, allowing realistic wear data to occur over a small number of holes.

3.2 Tool

To facilitate temperature measurements of cutting faces throughout the drilling process, whilst avoiding the use of slip rings etc., a setup was devised where the tool remained stationary and the sample was held and rotated in the CNC machine spindle.

The tools used were standard 8.9mm diameter, 118° point angle, high speed steel (HSS) twist drills, shown in Figure 2. A 1 mm diameter hole was spark eroded from the drill flank through to the flute (Figure 3a), in which a k-type thermocouple was cemented close to the flank surface using thermocouple cement (Omegabond High Temperature cement). The k-type thermocouple was selected for its small size (0.6mm) and the thermocouple cement provides both mechanical attachment and thermal conductivity. The cable was routed down the flute and secured using a Loctite Hi-Temp RTV silicone adhesive to provide protection against cable erosion during drilling. A flat was machined on the drill shank to allow mounting of the AE sensor (Figure 3b). In practical use sensors would likely be coupled to the stationary part but here the sample rotates to facilitate temperature measurements. Comparison with previous data from a sample mounted sensor

demonstrated that similar data was acquired in this configuration. Drills were mounted into a collet that is attached to a force dynamometer (Figure 3c).

3.3 Instrumentation and Data Acquisition

Thrust force was measured by a Kistler 9257BA force dynamometer coupled to an AD 5233AI amplifier (Figure 3c) and logged at 1000Hz sample rate throughout the drilling process. The thermocouple measuring tool temperature was connected to an Omega CNI3253 thermocouple amplifier and was logged using a National Instruments USB 6008 Data Acquisition Device (NI-USB 6008 DAQ) with a 5 Hz sample rate throughout the drilling process.

AE signals were recorded by a Mistras Group Ltd. Pico AE sensor (200-750 kHz). The sensor was mounted to the flat on the tool shank using cyanoacrylate adhesive which also provides acoustic coupling. A Mistras Group Ltd In-line amplifier (40dB Gain, 20-1200kHz) was used and signals were recorded by a Mistras Group Ltd. PCI-Express 8 acquisition system. The sensor output was also sampled continuously at 2 MHz (a continuous 'wavestream') for 10s, capturing the duration of the whole drilling process. Correct sensor installation was assessed using the Hsu-Nielsen pencil lead fracture technique (ASTM E976). A schematic of the measurement chain for all sensors is given in Figure 4.

Surface roughness measurements were taken using a Taylor Hobson Talysurf surface profilometer (stylus tip radius of 2 μ m and arm length of 6mm). The profiles were measured along the hole surface parallel to the drilling direction at a point on the hole circumference corresponding to the 0° direction (as per inset in Figure 8). Profiles started from the exit side and moved towards the entry

side. No filtering was applied in order to highlight the waviness that occurs due to variation in cutting performance.

Hole size was measured using a digital Vernier calliper and an average of 4 measurements was taken.

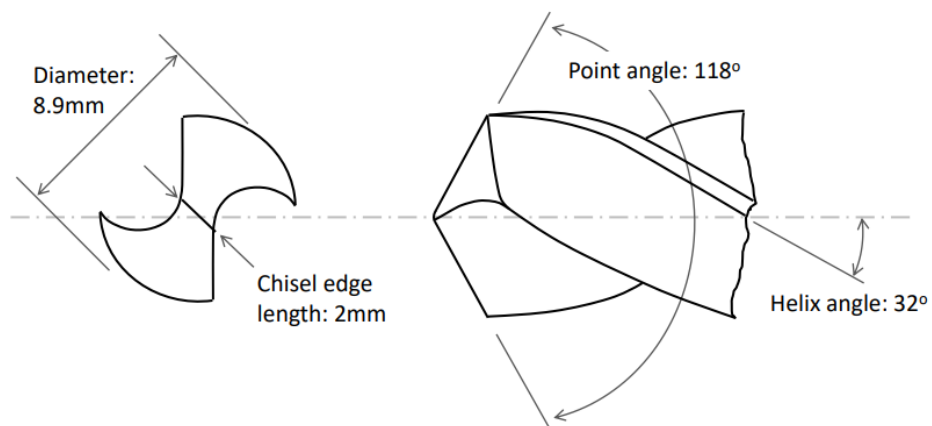


Figure 2: Drill geometry

3.4 Workpieces

Composite samples were manufactured from Cytac MTM28-1/T800H/12(k)/120/40%RW carbon fibre epoxy using a 28 ply $[(0/90/90/0/\pm 45)_2 / 0/90]_s$ quasi-isotropic layup. A 300 x 300mm panel was autoclave manufactured in line with manufacturer recommended cure cycles and the cured panel thickness was measured to be 3.95mm. Samples of 25 x 25mm were cut for testing and were mounted in a square pocket machined in the sample holder. Washers at the midpoint of two parallel sample edges were clamped in place by screws to secure the sample (Figure 3c). Full support of

the sample was provided with the exception of a 10mm diameter clearance hole to allow full breakthrough of the 8.9mm diameter drill. The holder was mounted in the head of a 3-axis milling machine which controlled the rotation and feed rate.

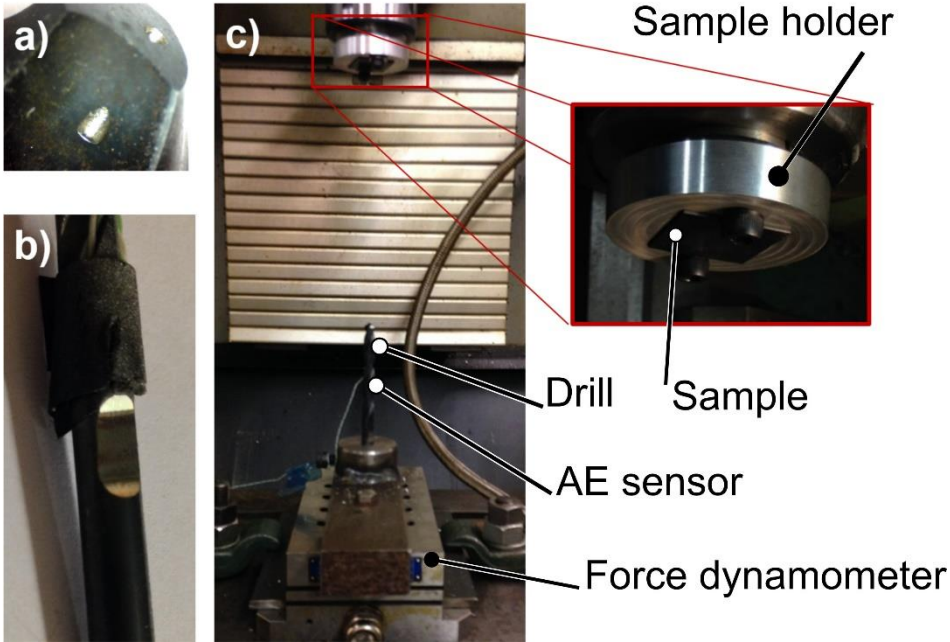


Figure 3: Experimental setup: a) thermocouple mounting position, b) sensor mounting position and c) drilling setup

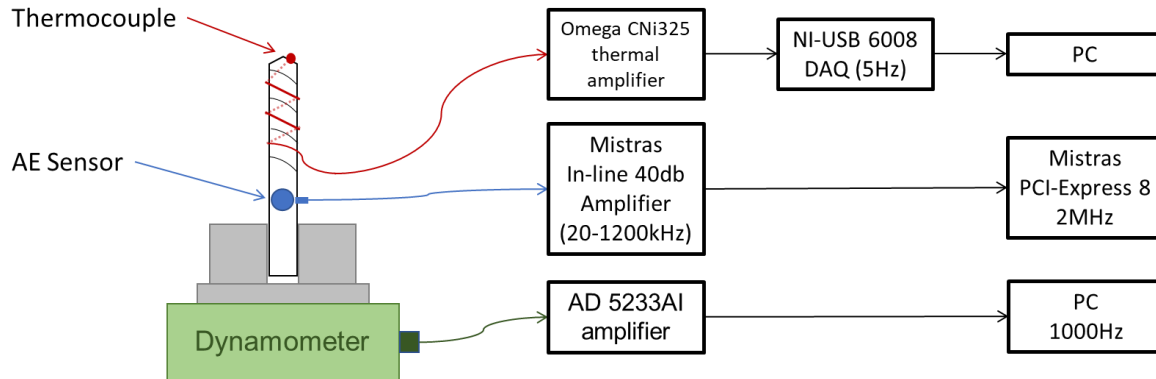


Figure 4: Schematic of measurement chain

3.5 Cutting Conditions

The cutting conditions are detailed in Table 1. The RPM remained constant at 1573 RPM (~26Hz) for all experiments and two feed rates of 0.0508 and 0.0326 mm/rev were assessed. A new HSS bit was used for each cutting condition and 8 holes were drilled at each feed rate (shown to produce considerable tool wear). A new CFRP sample was placed in the sample holder prior to drilling each hole and the tool temperature was returned to ambient between successive holes. A damp cloth was used to accelerate cooling of the tool. Thrust force, AE data and tool temperature were recorded simultaneously throughout the drilling of each hole.

Table 1: Parameters of Drilling Experiments

	Spindle Speed (RPM)	Feed Rate (mm/rev)	Number of Holes Drilled	Sample IDs
Condition 1	1573	0.0508	8	A-H
Condition 2	1573	0.0326	8	I-P

3.6 Outline of data analysis

A schematic overview of the data analysis approach is given in Figure 5. The example ‘wavestream’ in Figure 5a shows a variation in signal amplitude (or bursts). The occurrence frequency of the AE bursts (which can be considered as a carrier frequency) is expected to be closely related to the fibre cutting process. To enable analysis of the burst occurrence frequency, the analytical envelope of the signal is computed as the absolute value of the signal’s Hilbert transform (Figure 5b). It is important to note that the lower carrier frequency would not be detected without the use of higher frequency acquisition required to capture AE bursts. A short time frequency transform (STFT) of the enveloped signal is then calculated (Figure 5c) using a sliding gaussian window of 0.5s width and with a 90% overlap. This corresponds to a 2 Hz frequency resolution. Minor variations in tool speed are absorbed at this resolution, whilst different cutting frequencies are still resolved. The window width and overlap allows the correct capture of the various transient phases of cutting (i.e. initial tool contact, steady state cutting and tool exit) without losing temporal resolution.

The STFT identifies bands of high AE activity at frequencies corresponding to 2×RPM, 4×RPM and 8×RPM, which are related to the pass rate of the two cutting faces passing through multiple ply

orientations at any given time (a more in-depth explanation of cutting face pass frequencies is provided in the discussion section). The energy within a given frequency band is extracted with time (Figure 5d). This allows the maximum energy to be identified and the energy across time to be plotted against thrust force, highlighting the relationship between AE and thrust force (or tool wear). Variations in cutting and tool conditions can then be studied.

For comparison the conventional rolling RMS of the raw signal is calculated for a 0.5ms window with no window overlap. The maximum value achieved during a drilling process is recorded and compared to the hole number and the error in the hole diameter.

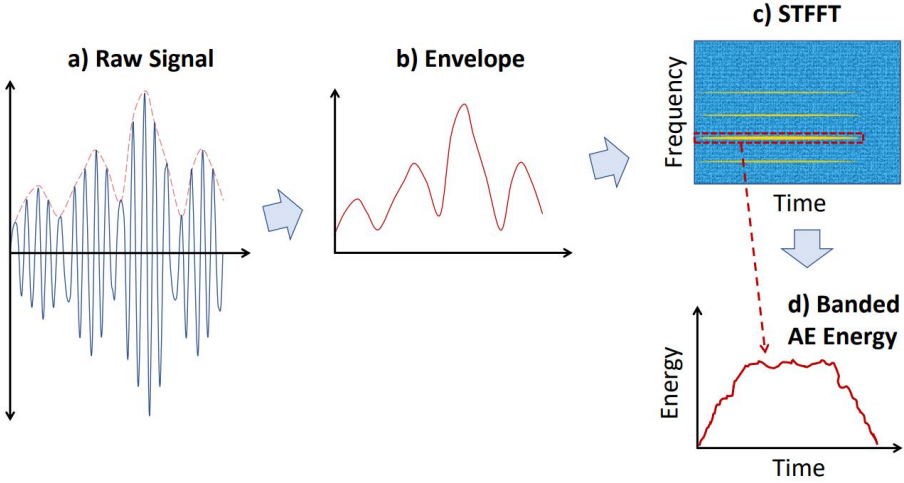
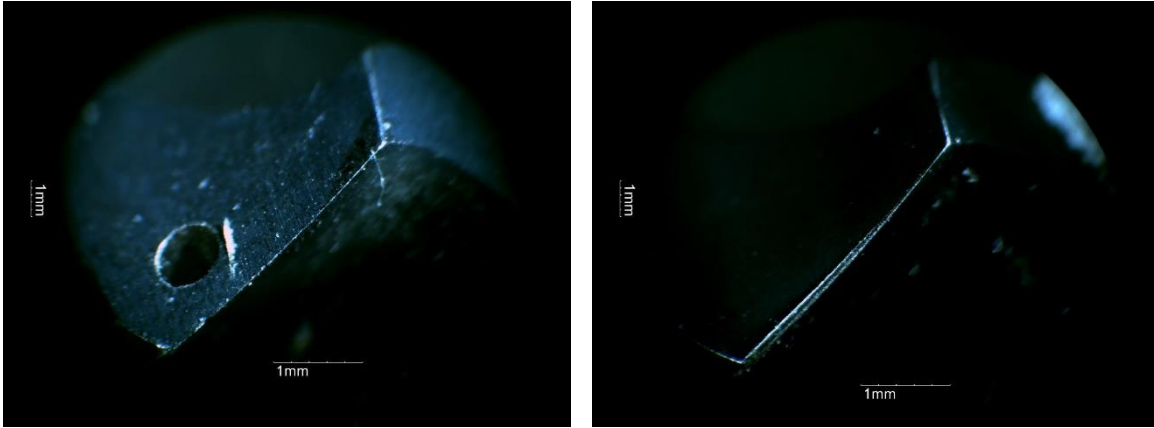


Figure 5: Schematic of data processing methodology a) Raw signal containing temporal bursts b) the analytical envelope (Hilbert transform) of the raw signal c) STFFT of signal envelope d) frequency banded energy

4 Results and discussion

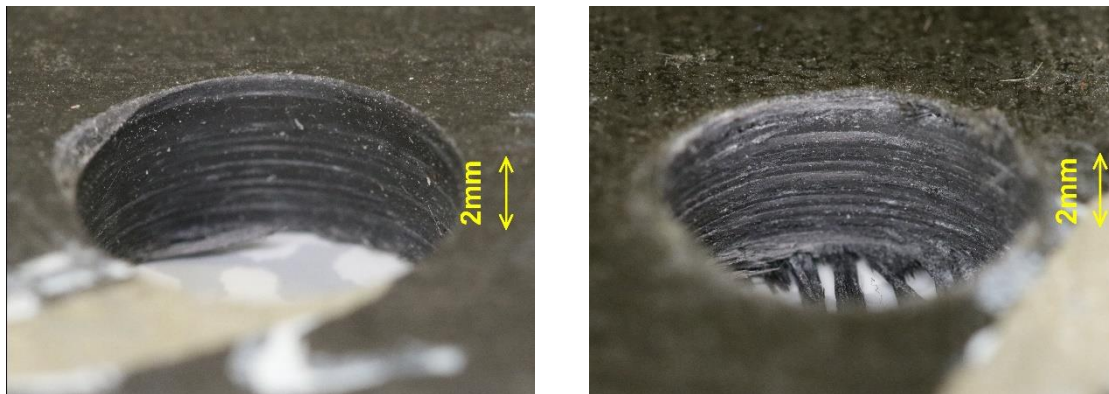
Figure 6 presents microscope images of a new drill (Figure 6a) and a drill after 8 hole drilling operations (Figure 6b). Qualitatively the cutting edge of the drill shows a broadening, in line with the expected increase in cutting edge radius (seen as a larger reflective/silver coloured area along the cutting edge in Figure 6b). This broadening gradually increases towards the outer circumference, in line with the increase in cutting distance experienced. This corresponds to a macroscopically observed degradation in hole quality, with Figure 7b showing burr formation at the hole entry, a rougher inner surface and an exit hole with fibre push-out rather than cutting. All of which are expected outcomes of CFRP drilling with a worn tool. Burr formation has been strongly linked with an increase in CER [54,55], i.e. tool wear. The fibre push out occurs when tool wear increases, leading to increased thrust force which subsequently pushes the last few layers outwards. It is likely that this fibre push out at the exit is accompanied by delamination, however, this will be somewhat limited by the support given by the fixture and has not been investigated further as it is not the focus of this study. The image of the used tool (Figure 6b) and the hole drilled with it (Figure 7b) both exhibit the expected behaviour of a worn tool, indicating that significant wear has occurred throughout the 8 holes drilled.



(a)

(b)

Figure 6: New drill (a) and drill after 8 holes (b). The used drill shows qualitative evidence of cutting-edge wear (reflective/silver coloured area).



(a)

(b)

Figure 7: sample A, cut by a new drill (a), and sample H, 8th hole cut (b). Sample H shows a rougher machined surface and fibres pushed out at the exit (feed rate: 0.0508 mm/rev).

Figure 8 shows the surface roughness profiles from holes A (new drill) and H (8th hole), where noticeably greater waviness is seen for sample H compared with sample A. The period of observed waviness in sample H is comparable to the ply thickness and occurs due to ineffective fibre cutting at different angles through the laminate thickness. The Ra, Rz and Rz,max values are presented in Table 2. Interpretation of roughness parameters must be considered carefully in fibre reinforced composites [56]. The Ra value represents the arithmetic mean of the magnitude of the deviation of the profile from the mean line. This averaging can make the Ra value insensitive to the localized peaks and valleys associated with fiber tear out and delamination cracks, hence the lower values observed (Table 2). The Rz value determines the maximum peak to valley height in a given sample length and averages across all sample lengths making up the total evaluation length. It is therefore more sensitive to the peaks and valleys associated with fiber tear out and delamination cracks as is evident by the larger magnitudes calculated compared with Ra in Table 2. However, the peaks and valleys of surface damage often occur over a length scale that is shorter than the sample length and they may only be present in a small number of sample lengths, meaning averaging still reduces sensitivity to such features. For this reason Teicher et al [56] suggest that Rz,max or Rt are better suited to assessing fiber reinforced materials. For Rz,max the difference between highest peak and lowest valley is determined for each sample length, the largest value recorded is then reported as the Rz,max value. For Rt the difference between the highest peak and the lowest valley for the entire evaluation length is taken. Here Rz,max is used and as expected it returns a larger value than both Ra and Rz (Table 2). An increase in Rz,max (115%) suggests the severity (size) of fiber tear out and delamination/cracking has increased, whereas the larger increases in Ra and Rz (133% and 152%, respectively) suggests the occurrences of fiber tear out and

delamination/cracking has increased. This corresponds to the qualitative observations made from the sample images (Figure 7) and raw roughness profiles (Figure 8).

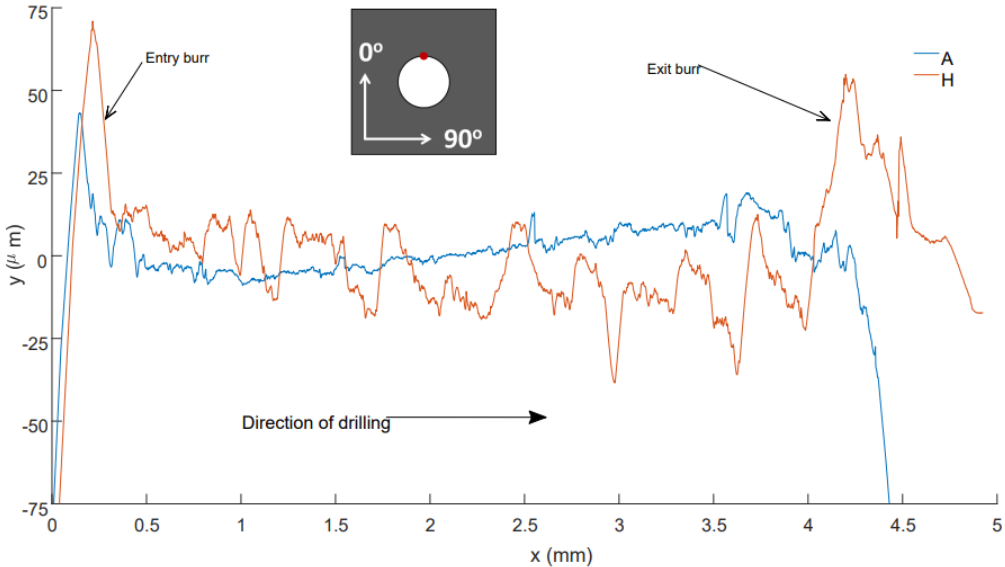


Figure 8: Profiles of hole surface obtained from sample A (new drill) and sample H (8th hole drilled by same drill). Sample H shows sharp jumps compatible with the position of different layers in the stack. Inset shows circumferential position where profiles were collected.

Table 2: Roughness values for samples A and H. The sampled length used to calculate these parameters excludes the entry and exit burrs.

Sample	Ra (μm)	Rz,max (μm)	Rz (μm)
A	2.97	22.95	13.59
H	6.92	49.20	34.30
% Increase from A→H	133%	114%	152%

The maximum thrust force recorded during the drilling of each hole is shown in Figure 9, for both feed rates (samples A→H represent holes 1 to 8, drilled at a feed rate of 0.0508 mm/rev; samples I→P represent holes 1 to 8, drilled at a feed rate of 0.0326 mm/min (Table 1)). The thrust force increases monotonically with increasing number of holes drilled at both feed rates. The thrust force is widely reported to strongly correlate to tool wear, confirming that significant wear occurs across the 8 holes drilled (thrust force increases by >50% after 8 holes, at both feed rates). Increases in thrust force were also observed for the second holes drilled at both feed rates, suggesting that significant tool wear occurs during the first hole drilled. Higher thrust forces also occur at higher feed rates (A→H), as expected.

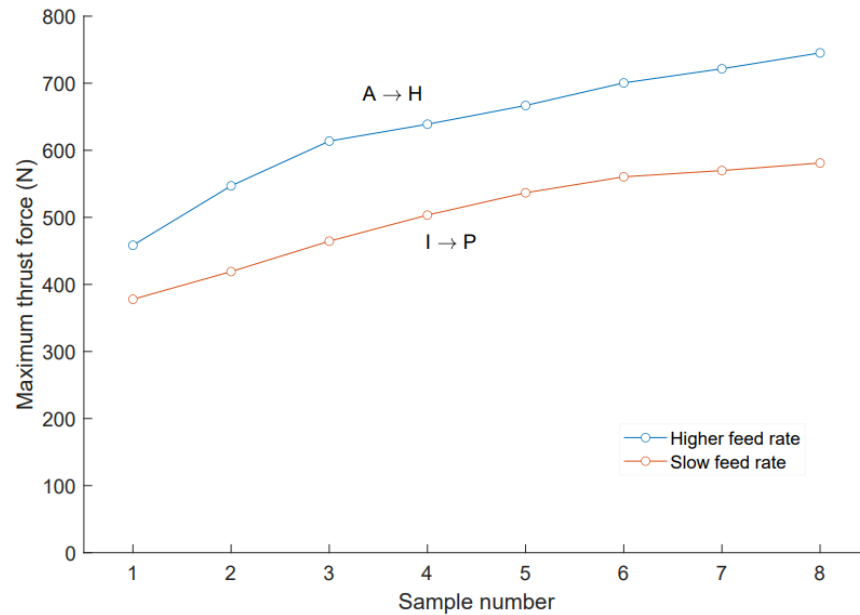


Figure 9: Peak thrust force for both datasets. As the number of holes drilled increases, the thrust force increases; high feed rates (A-H) also generate higher thrust forces.

The drill temperatures recorded during each test are presented in Figure 10 (samples A and B (higher feed rate) are missing due to issues with thermocouple data logging). Based on correlation between the two feed rates it is expected that these two tests would be at least 10-20°C cooler than the first two holes drilled at the lower feed rate, which were ~100°C and ~135°C, respectively.

In all cases, the maximum temperature recorded increases with number of holes drilled, further confirming tool wear is occurring. Peak temperatures reached at higher feed rates remain below those at lower feed rates, corresponding to longer cutting times at lower feed rates.

Following the first hole drilled, temperatures exceed the glass transition temperature (t_g) of the MTM28-1 resin system (reported by manufacturers to be 100°C (measured as the E' onset from DMA testing)). Above this temperature the resin will experience a significant loss in mechanical properties. This means that fibres will not be as well supported during cutting and the resin will not experience brittle fracture. Hence it is likely a change in the cutting regime will occur above this temperature.

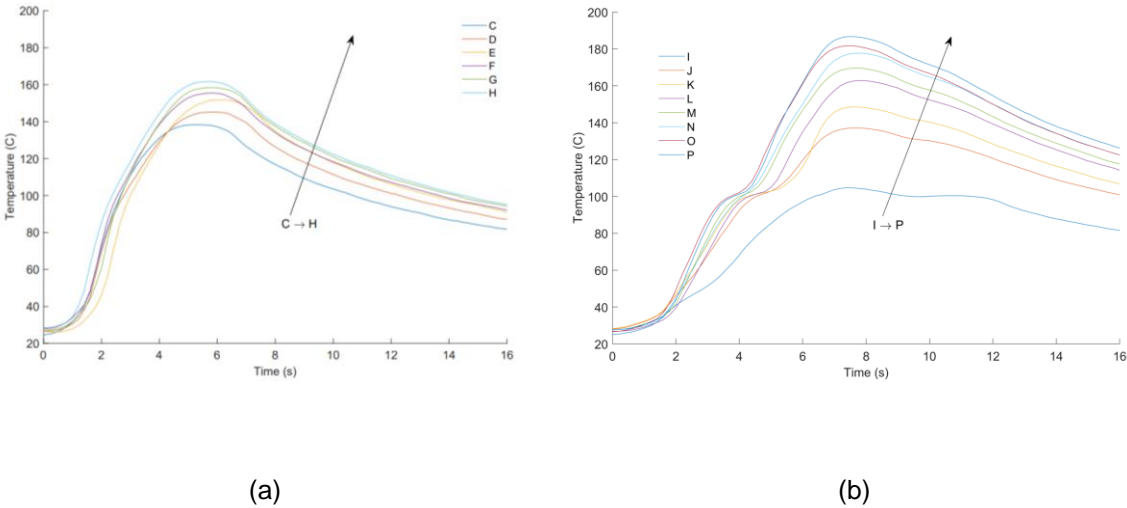


Figure 10: Temperature data during drilling for high feed rate (a) and low feed rate (b). Slower feed rates result in overall higher maximum temperatures. Temperature increases with the number of drilled holes.

Figure 11 presents an example of the raw data recorded during the drilling experiments. It shows how the AE wavestream, the thrust force and the temperature change with time for a new (a) and worn (b) tool. The AE signal amplitude is seen to reduce for the worn tool (in line with reports in the literature), as the thrust force and temperature increase. Figure 12 presents maximum rolling RMS (extracted from the raw AE wavestreams) versus a) number of holes drilled and b) measured hole diameter for both feed rates (note the x-axis in Figure 12b is inverse, i.e. hole size reduces moving rightwards). It can be seen from Figure 12b that cutting at the higher feed rate (Samples A-H) seems less effective, with the hole diameter reduced to ~8.85mm for the first hole, for a nominal drill diameter of 8.9mm. The maximum RMS levels of the AE signals are higher at the high feed rate (due to greater material removal per revolution) and the RMS values decrease monotonically as process quality deteriorates for both feed rates. As discussed in section 2.2 this is somewhat counterintuitive as poor cutting, leading to poor hole quality, would conventionally be expected to increase released AE energy.

The authors propose that this is linked to the T_g of the matrix and the high tool temperatures observed. With a new tool brittle chip formation occurs which is conducive to the release of high frequency AE energy, and a lack of rubbing or friction means the temperature remains lower. As the wear process evolves, greater friction and rubbing occur due to rounded cutting edges; resulting in increased temperature that softens the matrix. Material is then removed by a ploughing, or 'smearing', cutting regime. This means that fibres are not as well supported, so can be more readily pulled out at certain cutting angles (creating low spots) and bent over at other cutting angles (causing spring back and therefore high spots). This effect is clearly visible in the surface profile for sample H in Figure 8. This also explains the reducing hole size measured, as the Vernier calliper

will measure between the high spots resulting from fibre spring back (an effect reported by Poulachon et al and Wang et al [33,57]).

Figure 12 shows a large reduction in AE RMS over the first few holes drilled. This is very important, as it shows great sensitivity to the early stages of wear. Indeed, Figure 12b shows that over the first 4-5 holes drilled significant reductions in AE RMS (~50%) occur with small changes in hole diameter (<0.1mm). This is very promising from a tool condition monitoring perspective.

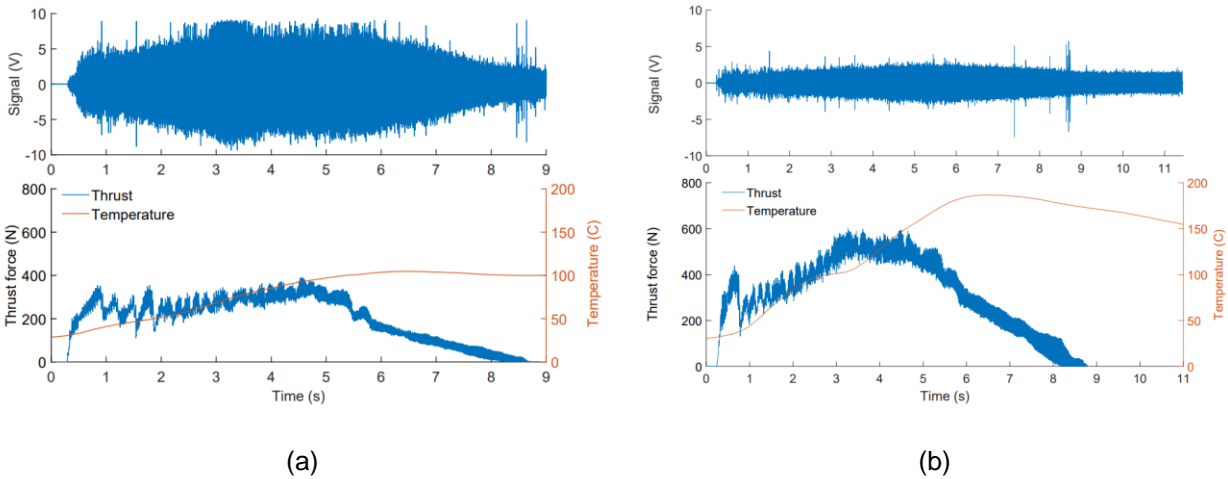


Figure 11: AE signals, forces and tool temperature for a new drill (a) and a worn drill (b). With the worn drill, the AE signals are globally weaker and both temperature and force are higher.

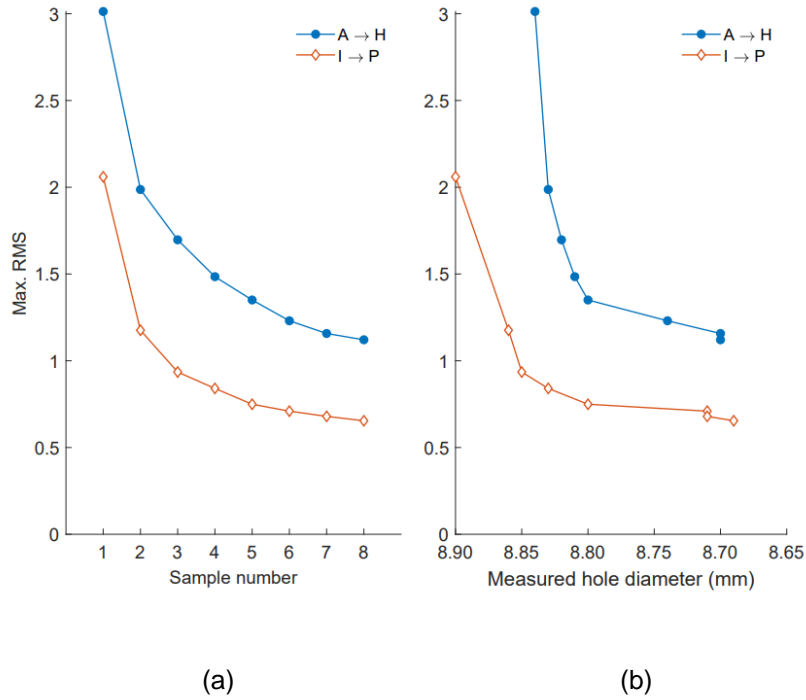


Figure 12: RMS of the AE signal against sample number (a) and measured hole diameter (b). As the RMS decreases, the hole quality degrades (note x-axis in (b) is inverse).

Figure 13 presents the STFT spectra of the enveloped AE wavestream for samples A to H (higher feed rate). Bands of energy can be seen at approximately 25Hz, 50Hz, 100Hz, 150Hz and 200Hz and remain present throughout the drilling process. These frequency bands represent the occurrence of lower frequency variation in AE signal amplitude, as shown schematically in Figure 5a and b. These frequencies are attributed to the tool rotation speed (~26Hz), the tool geometry (i.e. two cutting edges) and the cutting dynamics in fibre reinforced laminates as follows. In a

unidirectional laminate the cutting behaviour will change when cutting parallel to, perpendicular to or at an angle to the fibres [57–59]. This causes a fluctuation in the AE energy released, dependent on drill orientation at any given point in time. There are two cutting edges cutting at any given time and the quasi-isotropic layup means fibres are being cut in multiple directions at any given time. This leads to the higher order “harmonics” observed (i.e. 50Hz, 100Hz, 150Hz and 200Hz) which are all multiples of the fundamental tool rotation speed. This confirms that the variation in wavestream amplitude (i.e. bursts) correlates to the cutting process as hypothesised above. Some broad band activity is also observed at tool entry and exit, where more complex mechanisms are at play. Data for the lower feed rate are similar to those presented in Figure 13 for the higher feed rate. The same frequency bands are observed due to the same rotation speed and slightly lower amplitudes are seen due to lower feed rate. These figures are not included for brevity.

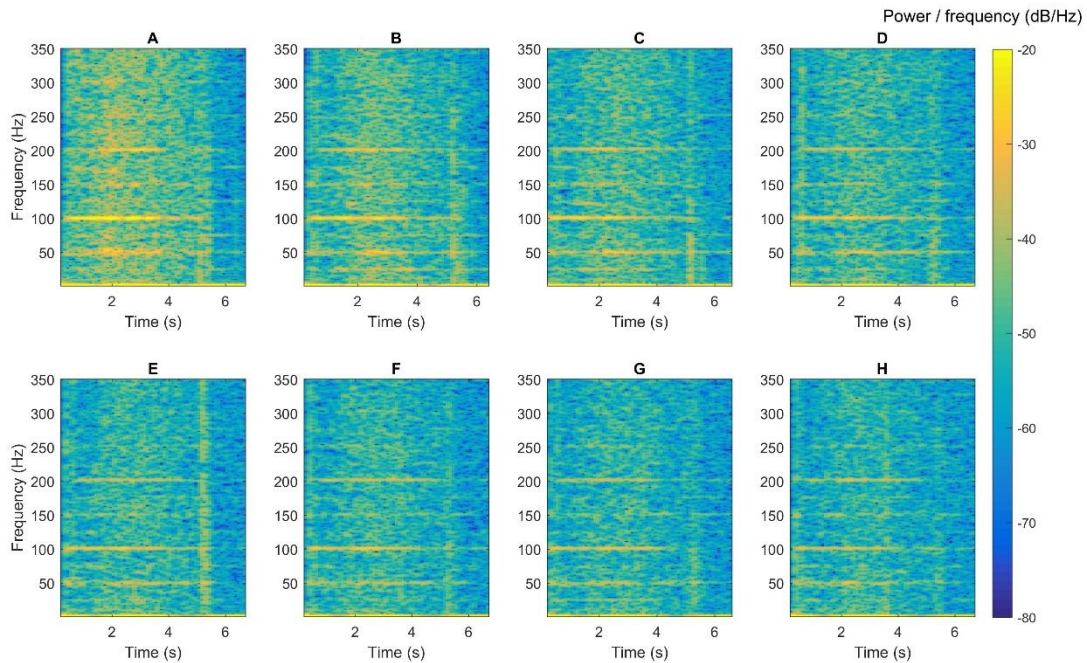


Figure 13: Spectrograms of AE envelope for higher feed rate. The ply cutting frequencies are clearly visible throughout all tests. Initial and final drilling breakouts are visible as a more broadband activity.

The 100Hz frequency band consistently demonstrates the highest energy in all signals in Figure 13, hence energy between 100 ± 2 Hz is investigated further. Figure 14 shows the AE energy collected in the 100Hz band throughout the drilling process plotted against thrust force for both feed rates. As seen from Figure 11a and b, the thrust force increases gradually to a maximum through the first phase of the process (as more cutting face engages) and then reduces gradually in the later part of the process (as tool breaks out). Consequently, this forms a loop in the data in Figure 14 where the

thrust force increases and then returns to zero. The shape of the loop is governed by the AE energy recorded, i.e. the more energy the more the loop stretches out to the right in the plot. As this is a dynamic and transient process the curves are slightly irregular in shape. The peak thrust force achieved for each sample gives an indication of tool condition, i.e. higher thrust force correlates to higher tool wear, with the thrust force (and therefore wear) increasing with each sample. The change in the peak value of banded AE energy achieved for each sample gives an indication of how sensitive this new metric (i.e. the 100 Hz frequency banded energy of a windowed AE wavestream) is to the tool wear that is occurring (indicated by increasing thrust force, temperature and surface roughness). A clear trend is evident that as the tool wears and the thrust force increases the banded AE energy reduces. This behaviour is consistent across both datasets.

For comparison to the conventional RMS analysis (presented in Figure 12), Figure 15 plots the peak banded AE energy against a) hole number and b) measured hole diameter. As with the RMS data, large reductions in banded AE energy are seen over the first 4-5 holes where minimal changes in hole quality are observed. Importantly the change observed in the banded AE energy is proportionally much greater than that of the RMS. The maximum banded AE reduces to 16% and 23% of the first hole value over the experiment, for the higher and lower feed rates, respectively. Comparatively, the RMS of the raw AE signal reduces to 31% and 42% of the first hole value for the highest and lowest feed rates, respectively. Other studies that have looked at the reduction in RMS of the raw AE signals with wear, have seen reduction to ~40% [20], ~ 30% [21], and 57% [44] of the level of the first hole drilled. This demonstrates the benefit and the significantly improved sensitivity of the proposed signal processing approach. This is achieved by focussing on the extraction of the

lower frequency temporal features in the raw AE signal (by enveloping) and therefore the energy released only by the cutting process can be capture and interpreted.

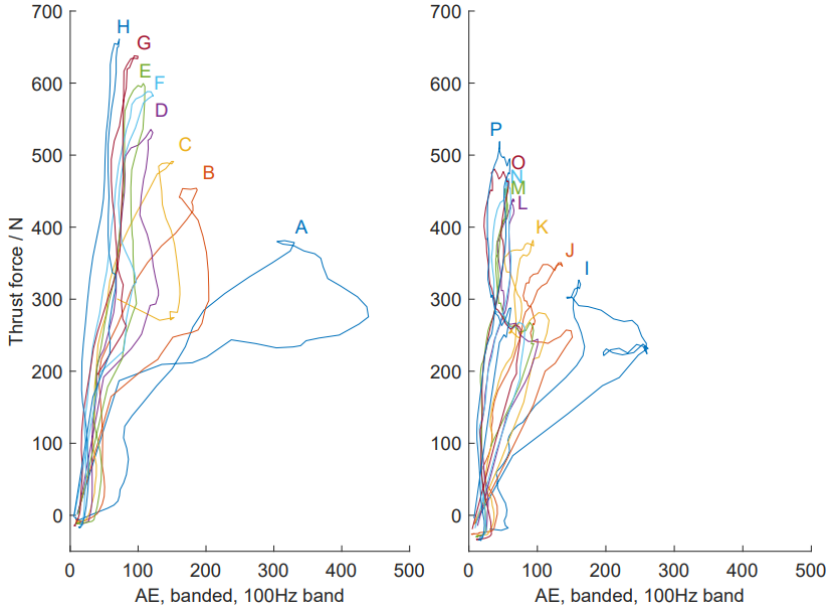


Figure 14: Thrust force versus banded energy of enveloped AE signal at the 100Hz peak. A new drill has high AE and low thrust force; as the thrust force required to feed the tool increases, the AE levels decrease.

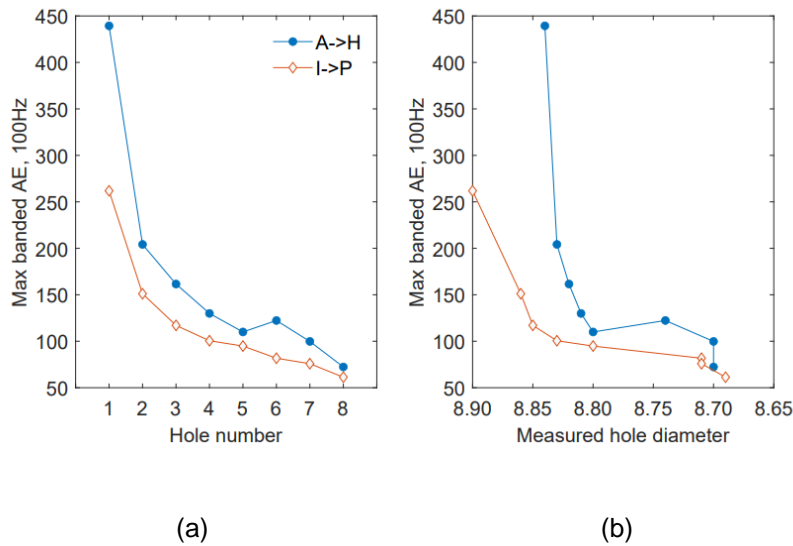


Figure 15: Maximum banded AE energy around 100Hz peak versus hole number (a) and measured hole diameter (b).

5 Conclusions

Continuous AE data was successfully recorded from a series of drilling experiments, in which the tool was shown to experience significant wear (via increased thrust force, increased tool temperature and reduced hole quality). The AE signal RMS level was shown to reduce with increasing tool wear, which is in line with previous studies. It was shown here for the first time that this reduction in RMS results from a change in the cutting regime brought about by the increased temperatures, which exceed the matrix t_g and lead to less brittle fracturing and more smearing/ploughing cutting mechanisms.

A new enveloping approach to data analysis was successful in capturing the lower frequency temporal features of the continuous AE wavestreams. Frequency analysis of the enveloped AE wavestream revealed that the lower frequency temporal features are related to the rotational speed of the tool. Capturing the data this way ensures that only AE released by cutting is considered and hence a more sensitive detection of changes in tool wear and therefore process conditions was demonstrated. Isolating the dominant 100Hz frequency band allowed a clear identification of changes in the cutting regime in these tests.

Based on these findings, there is potential to utilize information extracted from AE data as part of a system for a tool monitoring during composite machining. To make such a system practical, further investigation on sensor placement, differing layups, tool geometry, tool material and a greater range of cutting parameters is needed.

6 Acknowledgements

The authors would like to acknowledge the support of the technician staff at Cardiff School of Engineering for their help with the experimental setup. Thanks is also given to Paul Prickett from Cardiff School of Engineering for his support with instrumentation for thrust force acquisition, and to William Britton for assisting with the surface profilometry.

This research did not receive any specific grant funding from agencies in the public, commercial, or not-for-profit sectors.

7 References

- [1] Composites Leadership Forum. Lightening the Load: The 2016 UK Composites Strategy. 2016.
- [2] Airbus. A350 Family Aircraft. <https://www.airbus.com/aircraft/passenger-aircraft/a350xwb-family.html> 2021.
- [3] Boeing. 787 Dreamliner by Design. <https://www.boeing.com/commercial/787/by-design/#/advanced-composite-use> 2021.
- [4] Caggiano A, Nele L. Comparison of drilled hole quality evaluation in CFRP/CFRP stacks using optical and ultrasonic non-destructive inspection. *Machining Science and Technology* 2018;22. <https://doi.org/10.1080/10910344.2018.1466330>.
- [5] Abrão AM, Faria PE, Rubio JCC, Reis P, Davim JP. Drilling of fiber reinforced plastics: A review. *Journal of Materials Processing Technology* 2007;186. <https://doi.org/10.1016/j.jmatprotec.2006.11.146>.
- [6] Liu D, Tang Y, Cong WL. A review of mechanical drilling for composite laminates. *Composite Structures* 2012;94. <https://doi.org/10.1016/j.compstruct.2011.11.024>.
- [7] AMRC. Personal Communication 2017.
- [8] Faraz A, Biermann D, Weinert K. Cutting edge rounding: An innovative tool wear criterion in drilling CFRP composite laminates. *International Journal of Machine Tools and Manufacture* 2009;49. <https://doi.org/10.1016/j.ijmachtools.2009.08.002>.

- [9] Jantunen E. A summary of methods applied to tool condition monitoring in drilling. *International Journal of Machine Tools and Manufacture* 2002;42. [https://doi.org/10.1016/S0890-6955\(02\)00040-8](https://doi.org/10.1016/S0890-6955(02)00040-8).
- [10] Ambhore N, Kamble D, Chinchankar S, Wayal V. Tool Condition Monitoring System: A Review. *Materials Today: Proceedings* 2015;2. <https://doi.org/10.1016/j.matpr.2015.07.317>.
- [11] Serin G, Sener B, Ozbayoglu AM, Unver HO. Review of tool condition monitoring in machining and opportunities for deep learning. *The International Journal of Advanced Manufacturing Technology* 2020;109. <https://doi.org/10.1007/s00170-020-05449-w>.
- [12] Kuntoğlu M, Aslan A, Pimenov DY, Usca ÜA, Salur E, Gupta MK, et al. A Review of Indirect Tool Condition Monitoring Systems and Decision-Making Methods in Turning: Critical Analysis and Trends. *Sensors* 2020;21. <https://doi.org/10.3390/s21010108>.
- [13] Zhu G, Hu S, Tang H. Prediction of tool wear in CFRP drilling based on neural network with multicharacteristics and multisignal sources. *Composites and Advanced Materials* 2021;30. <https://doi.org/10.1177/2633366X20987234>.
- [14] Caggiano A, Centobelli P, Nele L, Teti R. Multiple Sensor Monitoring in Drilling of CFRP/CFRP Stacks for Cognitive Tool Wear Prediction and Product Quality Assessment. *Procedia CIRP* 2017;62. <https://doi.org/10.1016/j.procir.2017.03.047>.
- [15] Möhring H-C, Eschelbacher S, Kimmelmann M. Material failure detection for intelligent process control in CFRP machining. *Procedia CIRP* 2018;77. <https://doi.org/10.1016/j.procir.2018.09.042>.

- [16] Gaugel S, Sripathy P, Haeger A, Meinhard D, Bernthaler T, Lissek F, et al. A comparative study on tool wear and laminate damage in drilling of carbon-fiber reinforced polymers (CFRP). *Composite Structures* 2016;155. <https://doi.org/10.1016/j.compstruct.2016.08.004>.
- [17] Guo D-M, Wen Q, Gao H, Bao Y-J. Prediction of the cutting forces generated in the drilling of carbon-fibre-reinforced plastic composites using a twist drill. *Proceedings of the Institution of Mechanical Engineers, Part B: Journal of Engineering Manufacture* 2012;226. <https://doi.org/10.1177/0954405411419128>.
- [18] Romoli L, Lutey AHA. Quality monitoring and control for drilling of CFRP laminates. *Journal of Manufacturing Processes* 2019;40. <https://doi.org/10.1016/j.jmapro.2019.02.028>.
- [19] Merino-Pérez JL, Royer R, Merson E, Lockwood A, Ayvar-Soberanis S, Marshall MB. Influence of workpiece constituents and cutting speed on the cutting forces developed in the conventional drilling of CFRP composites. *Composite Structures* 2016;140. <https://doi.org/10.1016/j.compstruct.2016.01.008>.
- [20] Eaton M, Pearson M, Byrne C, Prickett P, Pullin R, Holford K. Ensuring Drill Quality in Composite Materials using Acoustic Emission. 16th European Conference on Composite Materials, Seville, Spain: 2014.
- [21] Eaton M, Williams R, Bryne C. A Study of Composite Drilling Mechanisms using Acoustic Emission. 11th International Conference on Experimental Mechanics, Exeter, UK: 2016.
- [22] Merino-Pérez JL, Royer R, Merson E, Lockwood A, Ayvar-Soberanis S, Marshall MB. Influence of workpiece constituents and cutting speed on the cutting forces developed in the

conventional drilling of CFRP composites. *Composite Structures* 2016;140.

<https://doi.org/10.1016/j.compstruct.2016.01.008>.

- [23] Caggiano A, Angelone R, Napolitano F, Nele L, Teti R. Dimensionality Reduction of Sensorial Features by Principal Component Analysis for ANN Machine Learning in Tool Condition Monitoring of CFRP Drilling. *Procedia CIRP* 2018;78.
<https://doi.org/10.1016/j.procir.2018.09.072>.
- [24] Raj DS, Karunamoorthy L. Study of the Effect of Tool Wear on Hole Quality in Drilling CFRP to Select a Suitable Drill for Multi-Criteria Hole Quality. *Materials and Manufacturing Processes* 2016;31. <https://doi.org/10.1080/10426914.2015.1004713>.
- [25] Ramirez C, Poulachon G, Rossi F, M'Saoubi R. Tool Wear Monitoring and Hole Surface Quality During CFRP Drilling. *Procedia CIRP* 2014;13.
<https://doi.org/10.1016/j.procir.2014.04.028>.
- [26] Saoudi J, Zitoune R, Mezlini S, Gururaja S, Seitier P. Critical thrust force predictions during drilling: Analytical modeling and X-ray tomography quantification. *Composite Structures* 2016;153. <https://doi.org/10.1016/j.compstruct.2016.07.015>.
- [27] Jones R. *Mechanics of Composite Materials*. 2nd ed. Abingdon: Taylor & Francis Group; 1999.
- [28] Babu J, Sunny T, Paul NA, Mohan KP, Philip J, Davim JP. Assessment of delamination in composite materials: A review. *Proceedings of the Institution of Mechanical Engineers, Part*

B: Journal of Engineering Manufacture 2016;230.

<https://doi.org/10.1177/0954405415619343>.

- [29] Haeger A, Schoen G, Lissek F, Meinhard D, Kaufeld M, Schneider G, et al. Non-destructive Detection of Drilling-induced Delamination in CFRP and its Effect on Mechanical Properties. *Procedia Engineering* 2016;149. <https://doi.org/10.1016/j.proeng.2016.06.647>.
- [30] Babu J, Paul Alex N, Abraham SP, Philip J, Anoop B, Davim JP. Development of a comprehensive delamination assessment factor and its evaluation with high-speed drilling of composite laminates using a twist drill. *Proceedings of the Institution of Mechanical Engineers, Part B: Journal of Engineering Manufacture* 2018;232. <https://doi.org/10.1177/0954405417690552>.
- [31] Xu J, Li C, Mi S, An Q, Chen M. Study of drilling-induced defects for CFRP composites using new criteria. *Composite Structures* 2018;201. <https://doi.org/10.1016/j.compstruct.2018.06.051>.
- [32] Heidary H, Ahmadi M, Rahimi A, Minak G. Wavelet-based acoustic emission characterization of residual strength of drilled composite materials. *Journal of Composite Materials* 2013;47. <https://doi.org/10.1177/0021998312459869>.
- [33] Wang B, Gao H, Cao B, Zhuang Y, Zhao Z. Mechanism of damage generation during drilling of carbon/epoxy composites and titanium alloy stacks. *Proceedings of the Institution of Mechanical Engineers, Part B: Journal of Engineering Manufacture* 2014;228. <https://doi.org/10.1177/0954405413508117>.

- [34] Merino-Pérez JL, Royer R, Ayvar-Soberanis S, Merson E, Hodzic A. On the temperatures developed in CFRP drilling using uncoated WC-Co tools Part I: Workpiece constituents, cutting speed and heat dissipation. *Composite Structures* 2015;123. <https://doi.org/10.1016/j.compstruct.2014.12.033>.
- [35] Fu R, Jia Z, Wang F, Jin Y, Sun D, Yang L, et al. Drill-exit temperature characteristics in drilling of UD and MD CFRP composites based on infrared thermography. *International Journal of Machine Tools and Manufacture* 2018;135. <https://doi.org/10.1016/j.ijmachtools.2018.08.002>.
- [36] Sorrentino L, Turchetta S, Bellini C. In process monitoring of cutting temperature during the drilling of FRP laminate. *Composite Structures* 2017;168. <https://doi.org/10.1016/j.compstruct.2017.02.079>.
- [37] Angelone R, Caggiano A, Improta I, Nele L, Teti R. Temperature Measurements for the Tool Wear and Hole Quality Assessment During Drilling of CFRP/CFRP Stacks. *Procedia CIRP* 2018;67. <https://doi.org/10.1016/j.procir.2017.12.235>.
- [38] An Q, Chen J, Cai X, Peng T, Chen M. Thermal characteristics of unidirectional carbon fiber reinforced polymer laminates during orthogonal cutting. *Journal of Reinforced Plastics and Composites* 2018;37. <https://doi.org/10.1177/0731684418768892>.
- [39] Kim D, Ramulu M. Frequency Analysis and Process Monitoring in Drilling of Composite Materials. *Advanced Composites Letters* 2004;13. <https://doi.org/10.1177/096369350401300402>.

- [40] Kuntoğlu M, Sağlam H. Investigation of signal behaviors for sensor fusion with tool condition monitoring system in turning. *Measurement* 2021;173.
- [41] Hill E, Moore P, Miller R, editors. *Non-destructive Testing Handbook, Volume 6: Acoustic Emission Testing*. third. American Society of Non-destructive Testing; 2005.
- [42] Arul S, Vijayaraghavan L, Malhotra SK. Online monitoring of acoustic emission for quality control in drilling of polymeric composites. *Journal of Materials Processing Technology* 2007;185. <https://doi.org/10.1016/j.jmatprotec.2006.03.114>.
- [43] Ravishankar SR, Murthy CRL. Characteristics of AE signals obtained during drilling composite laminates. *NDT & E International* 2000;33. [https://doi.org/10.1016/S0963-8695\(99\)00059-6](https://doi.org/10.1016/S0963-8695(99)00059-6).
- [44] Ravishankar SR, Murthy CRL. Application of acoustic emission in drilling of composite laminates. *NDT & E International* 2000;33. [https://doi.org/10.1016/S0963-8695\(00\)00014-1](https://doi.org/10.1016/S0963-8695(00)00014-1).
- [45] Leng S, Wang Z, Min T, Dai Z, Chen G. Detection of Tool Wear in Drilling CFRP/TC4 Stacks by Acoustic Emission. *Journal of Vibration Engineering & Technologies* 2020;8. <https://doi.org/10.1007/s42417-019-00190-5>.
- [46] Gómez MP, Hey AM, Ruzzante JE, D'Attellis CE. Tool wear evaluation in drilling by acoustic emission. *Physics Procedia* 2010;3. <https://doi.org/10.1016/j.phpro.2010.01.105>.
- [47] Zarif Karimi N, Minak G, Kianfar P. Analysis of damage mechanisms in drilling of composite materials by acoustic emission. *Composite Structures* 2015;131. <https://doi.org/10.1016/j.compstruct.2015.04.025>.

- [48] Maillet E, Baker C, Morscher GN, Pujar V v., Lemanski JR. Feasibility and limitations of damage identification in composite materials using acoustic emission. *Composites Part A: Applied Science and Manufacturing* 2015;75.
<https://doi.org/10.1016/j.compositesa.2015.05.003>.
- [49] Eaton MJ, Holford KM, Featherston CA, Pullin R. Damage in Carbon Fibre Composites: The Discrimination of Acoustic Emission Signals using Frequency. *Journal of Acoustic Emission* 2007;25:140–8.
- [50] Mascaro B, Gibiat V, Bernadou M, Esquerre Y. Acoustic emission of the drilling of carbon/epoxy composites. *Forum Acusticum, Budapest, Hungary: 2005*, p. 2823–7.
- [51] Möhring H-C, Kimmelman M, Eschelbacher S, Güzel K, Gauggel C. Process monitoring on drilling fiber-reinforced plastics and aluminum stacks using acoustic emissions. *Procedia Manufacturing* 2018;18. <https://doi.org/10.1016/j.promfg.2018.11.008>.
- [52] Kimmelman M, Duntschew J, Schluchter I, Möhring H-C. Analysis of burr formation mechanisms when drilling CFRP-aluminium stacks using acoustic emission. *Procedia Manufacturing* 2019;40. <https://doi.org/10.1016/j.promfg.2020.02.012>.
- [53] Rimpault X, Chatelain J-F, Klemberg-Sapieha J-E, Balazinski M. Fractal Analysis of Cutting Force and Acoustic Emission Signals During CFRP Machining. *Procedia CIRP* 2016;46.
<https://doi.org/10.1016/j.procir.2016.03.171>.

- [54] Poór DI, Geier N, Pereszlai C, Xu J. A critical review of the drilling of CFRP composites: Burr formation, characterisation and challenges. *Composites Part B: Engineering* 2021;223:109155. <https://doi.org/10.1016/j.compositesb.2021.109155>.
- [55] Wang F-J, Yin J-W, Ma J-W, Jia Z-Y, Yang F, Niu B. Effects of cutting edge radius and fiber cutting angle on the cutting-induced surface damage in machining of unidirectional CFRP composite laminates. *The International Journal of Advanced Manufacturing Technology* Volume 2017;91:3107–20.
- [56] Teicher U, Rosenbaum T, Nestler A, Brosius A. Characterization of the Surface Roughness of Milled Carbon Fiber Reinforced Plastic Structures. *Procedia CIRP* 2017;66. <https://doi.org/10.1016/j.procir.2017.03.282>.
- [57] Poulachon G, Outeiro J, Ramirez C, André V, Abrivard G. Hole Surface Topography and Tool Wear in CFRP Drilling. *Procedia CIRP* 2016;45. <https://doi.org/10.1016/j.procir.2016.02.348>.
- [58] An Q, Ming W, Cai X, Chen M. Study on the cutting mechanics characteristics of high-strength UD-CFRP laminates based on orthogonal cutting method. *Composite Structures* 2015;131:374–83. <https://doi.org/10.1016/j.compstruct.2015.05.035>.
- [59] Wang C, Wen L, Ming W, An Q, Chen M. Experimental study on effects of fiber cutting angle in milling of high-strength unidirectional carbon fiber–reinforced polymer laminates. *Proceedings of the Institution of Mechanical Engineers, Part B: Journal of Engineering Manufacture* 2018;232:1813–24. <https://doi.org/10.1177/0954405416679868>.

